Histol Histopathol (2025) 40: 1185-1194

Histology and Histopathology
From Cell Biology to Tissue Engineering

ORIGINAL ARTICLE Open Access

Ultrastructural assessment of human periodontal ligament fibroblast interaction with bovine pericardium membranes: An *in vitro* study

Sara Bernardi, Enrico Marchetti, Diana Torge, Davide Simeone, Guido Macchiarelli and Serena Bianchi
Department of Life, Health and Environmental Sciences, University of L'Aquila, L'Aquila, Italy

Summary. Research towards regenerative dentistry focused on developing scaffold materials whose high performance induces cell adhesion support and guides tissue growth. An early study investigated the proliferation abilities and attachment of human periodontal ligament fibroblasts (HPLFs) on two bovine pericardium membranes with different thicknesses, 0.2 mm and 0.4 mm. Following those published results, we examined the ultrastructure of HPLFs in contact with these membranes. The HPLFs were cultured in standard conditions, exposed to the tested materials, and, after 24 hours, subjected to transmission electron microscopy preparation. The examined parameters included the quality and distribution of mitochondria, Golgi apparatus, and the nucleus. HPLFs exposed to membranes showed ultrastructural changes. The cellular compartments aimed at protein synthesis and metabolism increased compared with the control. Unpaired *t*-test and one-way ANOVA showed that HPLFs exposed to membranes displayed an increase in the number of mitochondria (89.23±7.44 vs. 66.90±9.58; T1 and control; $p<0.05$ and 84.05±14.01 vs. 66.90±9.58; T2 and control; $p<0.05$). The reported ultrastructural evidence suggests an active synthesis state of HPLFs, probably triggered by the bovine collagen membrane, showing an active role of this material in the biology of the regeneration process.

Key words: Regenerative dentistry, Biomaterials, Collagen membranes, Human periodontal ligament fibroblasts, Morphology, Transmission electron microscopy

Introduction

The need for adequate biomaterials for application in regenerative medicine and rehabilitation procedures leads to continuous and dynamic research on this topic. In particular, the field of regenerative dentistry has seen important advancements in the development of biomaterials (Mehta et al., 2018; Arjunan et al., 2021). These materials are particularly relevant in regenerative surgeries, such as sinus augmentation, ridge preservation, guided bone regeneration (GBR), and periodontal regeneration (Mehta et al., 2018).

Scientific research led to the evolution of biocompatible and multifunctional biomaterials, with unique and specific chemical (Bianchi et al., 2022a,b), mechanical, and biological properties (Mehta et al., 2018; Arjunan et al., 2021); particularly, cyto-compatibility and bioactivity due to the ability to interact with the tissue environment, activating a specific biological response (Mas-Moruno et al., 2019). This aspect has led to the development of bioactive biomaterials for tissue reconstruction, applied in different dental and medical contexts (Mas-Moruno et al., 2019).

These biomaterials are also called "scaffold" materials due to their ability to promote cell adhesion, stimulate specific protein synthesis, and provide support for the growth of the tissue (Arjunan et al., 2021). Physiological regeneration depends upon the clot's

Corresponding Author: Sara Bernardi, Department of Life, Health and Environmental Sciences, University of L'Aquila, 67100 L'Aquila, Italy. e-mail: sara.bernardi@univaq.it
www.hh.um.es. DOI: 10.14670/HH-18-860

Abbreviations. DDSA, dodecenyl succinic anhydride specially distilled; DMP-30, 2,4,6-Tri(dimethylaminomethyl) phenol; d-PTFE, dense-polytetrafluoroethylene; ECM, extracellular matrix; ER, endoplasmic reticulum; EU, euchromatin; e-PTFE, expanded-polytetrafluoroethylene; FBS, fetal bovine serum; FGS, fibroblast growth supplement; FM, fibroblast medium; GBR, guided bone regeneration; HE, heterochromatin; HPLFs, human periodontal ligament fibroblasts; LM, light microscopy; NMA, methyl-5-Norborene-2,3-Dicarboxylic Anhydride; OsO4, osmium tetroxide; PO, propylene oxide; rRNA, ribosomal RNA; SD, standard deviation; SEM, scanning electron microscopy; TEM, transmission electron microscopy

stability, and scaffold materials play an essential role in this process. Moreover, the membranes protect and stabilize the wound site, excluding epithelial and connective tissue cells from the area from being regenerated (Arjunan et al., 2021).

Two main categories of membranes are available for clinical use: non-resorbable and resorbable membranes. The non-resorbable membranes can be made of expanded-polytetrafluoroethylene (e-PTFE), dense-polytetrafluoroethylene (d-PTFE), titanium mesh, and titanium-reinforced PTFE (Soldatos et al., 2017). The primary advantage of non-resorbable membranes is their long-term stability. On the other hand, their main disadvantages are their difficulty in handling, the risk of infection if they are exposed to the environment (Mehta et al., 2018), and the primary fixation of the membrane in the first surgery, and a second surgical procedure for removal (Arjunan et al., 2021). Resorbable membranes are made of collagen proteins, which can derive from human (Mehta et al., 2018), porcine (Vallecillo-Rivas et al., 2021), or bovine pericardium (Shi et al., 2023), calfskin (Mehta et al., 2018), Achilles tendon (Huang et al., 2023), and dermis (Mehta et al., 2018). The main advantages of resorbable membranes are the low risk of infection and the lack of a second intervention for removal. Bovine pericardium membranes are resorbable and decellularized to remove antigenic epitopes, associated with cell membranes and intracellular components, and to enhance biocompatibility with the wound site (Mehta et al., 2018). The process preserves the three-dimensional structure of the collagen net, which is mainly type I collagen hierarchically organized in different levels with various structures, such as fibrils, fibers, fiber bundles, and laminates (Mendoza-Novelo et al., 2011), conferring to bovine pericardium a non-linear and anisotropic mechanical behavior (Zioupos and Barbenel, 1994), assuring good stability and handling.

Bovine pericardium membranes display functional and morphological potential and are fundamental for examining cellular behavior (Liu et al., 2016). Positive histological findings, reported by several studies, confirmed the application of bovine pericardium membranes in the dental and medical fields (Setyawati et al., 2020). Among them, recent studies have investigated the potential role of lyophilized bovine pericardium in periodontal ligament fibroblast attachment, migration, and proliferation (Athar et al., 2014). Other scientific evidence demonstrated the contribution of bovine pericardium membranes in the osteo-angiogenic differentiation process in periodontal ligament stem cells (Pizzicannella et al., 2019).

Moreover, bovine pericardium membranes are deeply involved in tissue regeneration as they enhance periodontal ligament fibroblasts, sustaining the proliferation and regeneration of osteoblasts, and providing a compatible microenvironment for the migration and proliferation of host cells (Elboraey and Mously, 2023). Recently, the bovine pericardium membrane was shown to be efficient for GBR for rabbit mandibular defects (Bai et al., 2014), however, before further clinical applications, *in vivo* studies on larger animals should be performed. If the *in vitro* and clinical studies carried out so far showed good compatibility for these grafts in GBR procedures, other studies highlighted how the clinical application in cardiological disciplines is still problematic due to the immune reaction of the recipient towards the xenogeneic biomaterials (Simon et al., 2003; Manji et al., 2006).

Indeed, the immune responses include the production of antibodies directed towards galactose-α-1,3-galactose (gal) and non-gal antigens (Griesemer et al., 2014), which limit the use and durability of the graft, and determine its rejection (Manji et al., 2015). It is crucial, therefore, to assess the effective surface antigens prior to clinical application to reduce the possibility of graft rejection (Gates et al., 2017).

This class of biomaterials is characterized by its acellularity, good consistency, excellent mechanical properties, and optimal thickness, which contribute to its regenerative potential in various cell populations, including human periodontal ligament fibroblasts (HPLFs) (Elboraey and Mously, 2023). HPLFs are a specific cell population of the periodontal ligament, used for *in vitro* periodontal regeneration model experiments. (Chang et al., 2023). Furthermore, they are involved in the attachment of the bone to the root surface by using collagen fibers. HPLFs are essential for the synthesis and degradation of collagen and can support osteoblast activity (Chang et al., 2023).

Despite their similar morphology to gingival fibroblasts (GFs), this cell population displays specific functional features in maintaining tissue integrity (Wang et al., 2020). Furthermore, HPLFs imitate osteoblast lineage cells by expressing important osteogenic markers, such as minerals, collagen, and alkaline phosphatase (Wang et al., 2020). HPLFs are deeply involved in the regenerative processes of periodontal tissues, at the same time, resorbable membranes are commonly used in regenerative dentistry and are often characterized by different thicknesses to modulate reabsorption and stabilize the healing site. Therefore, in clinical practice, these cells and membranes are routinely in contact (Mehta et al., 2018).

Understanding the impact of exposure to bovine pericardium membranes on the ultrastructure of HPLFs is a key focus of ongoing research. Therefore, transmission electron microscopy (TEM) can be useful for investigating ultrastructural changes (Burattini and Fancieri, 2013; Coaguila-Llerena et al., 2024) that occur within HPLFs when exposed to this class of regenerative biomaterials. The detailed understanding of the structural and ultrastructural profile of HPLFs, when exposed to regenerative biomaterials, might provide deeper insights into exploring the morpho-functionality of this cell population and defining their regulatory role in regenerative processes. This ultrastructural study

aimed to assess the effect of bovine pericardium membranes of varying thicknesses on the ultrastructure of HPLFs after 24-hour culture, using TEM. After 24 hours of cell culture, HPLFs were subjected to standard TEM preparation to analyze the following ultrastructural parameters: the ultrastructure of the nucleus, nucleoli, and the distribution of the endoplasmic reticulum (ER), Golgi apparatus, and mitochondria, which together provide a comprehensive ultrastructural profile of HPLFs in contact with the tested materials. Our null hypothesis was that there were no quantitative differences in the presence of mitochondria in cell cultures exposed to the membranes and in cultures of the control group.

Materials and methods

The study design included evaluating, using TEM, the ultrastructural profile of HPLFs cultured for 24 hours and unexposed to bovine pericardium membranes (control group). This control group is crucial as it provides a baseline for comparison. We also studied HPLFs in contact for 24 hours with bovine pericardium membranes (T1, thickness: 0.2 mm) and HPLFs exposed for 24 hours to bovine pericardium membranes (T2, thickness: 0.4 mm). Examinations were performed with three technical replicates.

Membranes

The membranes chosen for this study were derived from bovine pericardium and decellularized by the manufacturer (UBGEN Srl, Vigonza (PD), Italy). The three-dimensional structure of collagen is maintained according to the manufacturer's specifications. The assays were performed using two membrane thicknesses: T1-0.2 mm and T2-0.4 mm.

Cell culture

After thawing, the HPLF cell line obtained from Innoprot, Ltd (Bizkaia, Spain) was cultured according to the manufacturer's instructions (Bianchi et al., 2022a,b). The original vial containing 5×10^5 cells in 1 mL of volume, was cultured in three plastic culture dishes with fibroblast medium (FM - Innoprot, Bizkaia-Spain) and incubated under standard cell culture conditions (37°C in 5% CO_2). According to the manufacturer, a bottle of FM is composed of 500 mL of basal medium, 10 mL of fetal bovine serum (FBS, Innoprot, Bizkaia-Spain), 5 mL of fibroblast growth supplement (FGS), and 5 mL of penicillin/streptomycin solution (10,000 IU/mL of penicillin, 10 µg/mL streptomycin, Innoprot, Bizkaia, Spain) (Bianchi et al., 2022a,b). Once the cells reached sub-confluence, they were detached using 0.05% trypsin and subcultured at 110 cells/mm density. The cells were used at subculture passages 7 or 8 for all experimental assays and were exposed to bovine pericardium membranes (0.2 mm and 0.4 mm) for 24 hours.

TEM preparation

Sampling

Firstly, HPLFs were suspended in 1.5 ml of FM and centrifuged in a microcentrifuge at 1250 rpm for 5 minutes to obtain the cell pellets. The resulting HPLF pellets were carefully sampled and should be representative of the specimens.

The samples selected for ultrastructural analysis consisted of HPLF pellets divided into the following experimental groups: control (n=6), HPLFs exposed to bovine pericardium membranes with a thickness of 0.2 mm (T1, n=6) and HPLFs exposed to bovine pericardium membranes in contact for 24 hours with bovine pericardium membranes with a thickness of 0.4 mm (T2, n=6).

Primary fixation

Once HPLF pellets were obtained by centrifugation, samples were immersed in 2.5% Glutaraldehyde (Agar Scientific, Cambridge Road Stansted Essex, UK) in PBS for the primary fixation, then centrifuged at 1250 rpm for 5 minutes and stored at 4°C for 48 hours until the start of the embedding (Orioles et al., 2022; Torge et al., 2024).

Post-fixation

Forty-eight hours after primary fixation, HPLF samples were washed in cooled PBS (0.1 M, pH 7.2 - Immunological Sciences) to remove all primary fixative residues (three changes, thirty minutes each). After these washes in cooled PBS, HPLF pellets were then centrifuged at 1250 rpm for 5 minutes and post-fixed with 1% Osmium tetroxide (OsO_4) (Agar Scientific, Stansted, UK) in distilled water for 2 hours. During the post-fixation procedure, the HPLF pellets were completely black, suggesting that post-fixation procedures were completed.

Embedding

Once completed the post-fixation stage, HPLF samples were washed with cooled PBS (three changes, ten minutes each) to remove all the residues of OsO_4 and dehydrated in an ascending series of ethanol. Specifically, after removing all the residues of cooled PBS, HPLF pellets were dehydrated with ethanol 30% (one change for fifteen minutes), 50% (one change for fifteen minutes), 70% (one change for fifteen minutes), 95% (two changes, fifteen minutes each), and 100% (four changes, twenty minutes each). Once all the ethanol 100% was removed, samples were immersed in propylene oxide (PO - Electron Microscopy Sciences, 1560 Industry Road, Hatfield, PA, USA) for solvent substitution (two changes, thirty minutes each). Then, HPLF pellets were infiltrated overnight in PO/Epoxy

resin (1:1). On the day after, HPLF samples were embedded in the epoxy resin EMbed-812 (Electron Microscopy Sciences, 1560 Industry Road, Hatfield, PA, USA) for 2 hours. Then, samples were placed in the oven for 48 hours at 60°C to complete TEM preparation. According to the manufacturer, the epoxy resin EMbed-812 was composed of 20 ml of embedded resin, 16 ml of Dodecenyl Succinic Anhydride Specially Distilled (DDSA), and 8 ml of Methyl-5-Norborene-2,3-Dicarboxylic Anhydride (NMA) (Electron Microscopy Sciences, 1560 Industry Road, Hatfield, PA, USA). Finally, 770 µl of 2,4,6-Tri(dimethylaminomethyl) phenol (DMP-30) (Electron Microscopy Sciences, 1560 Industry Road, Hatfield, PA, USA) was added to the mixture, and the mix was gently resuspended.

Sectioning with the ultramicrotome

After heat polymerization for 48 hours at 60°C, the selected and embedded HPLF samples were removed from the oven and then sectioned using a Reichert–Jung Ultracut E ultramicrotome. Using a glass knife, samples were sectioned until pellets were revealed, and some semithin sections were cut. Semithin sections (1 µm thick) were stained with Methylene Blue (Agar Scientific), examined using light microscopy (LM) (Zeiss Axioskop, Zeiss, Oberkochen, Germany), and photographed using a digital camera (Leica DFC230, Wetzlar, Germany). The semithin sections, stained to varying degrees of blue, were then mounted with a new rapid mounting medium for microscopy, Neo-Mount® (Merck Millipore, Burlington, Massachusetts, United States). This procedure allowed us to analyze the morphology of HPLFs in contact with bovine pericardium membranes. After selecting appropriate areas of interest, the EPON block was trimmed for ultrathin sectioning. Ultrathin sections (60-80 nm) were then cut with a diamond knife (Diatome Diamond Knives, Microcontrol, Milan, Italy) and mounted on copper grids (Electron Microscopy Sciences, 1560 Industry Road, Hatfield, PA, USA).

UranyLess and lead citrate staining

The copper grids containing the ultrathin sections of HPLF samples were then stained with UranyLess and lead citrate 0.3% in distilled water (SIC, Rome, Italy). The samples were then examined and photographed using Philips TEM CM100 Electron Microscopes operating at 80 kV.

Morphometric and statistical analysis: Assessment of mitochondrial number

Mitochondrial counting was performed through a collection of low-magnification microphotographs of the control, T1, and T2 groups, examining all three technical triplets. The number of mitochondria was determined on at least three equatorial sections per group (distance between the sections: 3 µm), and ImageJ 1.54 v software was used to measure the number of mitochondria. Digital images were further enlarged to easily recognize and count mitochondria. Then, the number of mitochondria, expressed as the number of mitochondria per 100 μm^2 of the HPLF area, was calculated and expressed as mean ± standard deviation (SD) (Leoni et al., 2015; Murray et al., 2018). The statistical analysis was performed to determine the presence of significant differences between the means of independent samples. Statistical comparisons were performed employing an unpaired t-test and one-way ANOVA with Tukey's honest significant difference (HSD) tests for *post-hoc* analysis using GraphPad Prism 10.2.0 (GraphPad Software, San Diego, CA, USA). The null hypothesis was rejected if the p-value was <0.05 and the eventual differences were statistically significant. First, we collected the values of the means and SD of the selected experimental groups (control, T1, and T2) derived from mitochondrial counting. Then, after assessing the normal distribution of the data, an unpaired *t*-test and one-way ANOVA with Tukey's HSD tests for *post-hoc* analysis for multiple comparisons were performed to assess any significant variation between the considered follow-ups. Specifically, the unpaired *t*-test is a parametric statistical method used to test the hypothesis for comparison of means between two groups of independent samples. In this study, the values of the means and SD of two experimental groups were compared using the unpaired *t*-test to compute the significance level. ANOVA was used to compare the means among three or more groups. This omnibus statistic test compared values derived from mitochondrial counting, expressed as mean ± SD, to compute the significance level. Its significant p-value indicates at least one pair with a statistically significant mean difference. Furthermore, *post-hoc* tests were used to determine the significant pair(s) after ANOVA was significant: in this case, we performed one-way ANOVA with Tukey's HSD tests for *post-hoc* analysis as variances were homogeneous.

Results

The following ultrastructural parameters were examined using TEM in samples of HPLFs derived from the control, T1, and T2 groups: the ultrastructure of the nucleus and nucleolus, the distribution of heterochromatin (HE) and euchromatin (EU), the ultrastructure and distribution of mitochondria, the presence and quality of the ER and Golgi apparatus, and the ultrastructure and distribution of cytoplasmic projections.

Ultrastructure of HPLFs cultured for 24h: Control group

In the control group (Fig. 1A,B), HPLFs unexposed to bovine pericardium membranes displayed a large nucleus with a prominent nucleolus. Also, TEM observation highlighted the presence of HE, mainly localized in the periphery of the nucleus, while EU filled

most of the nucleus space. Clustered mitochondria and extensive cytoplasmic projections were also detectable in HPLFs unexposed to bovine pericardium membranes (Fig. 1A,B).

Ultrastructure of HPLFs cultured for 24h in the presence of membranes: T1 and T2 samples.

Ultrastructural observations in HPLFs exposed for 24h to bovine pericardium membranes (T1) highlighted the presence of a large nucleus with different prominent nucleoli (Fig. 2A,B). Moreover, HE was localized in the periphery of the nucleus, while EU filled most of the nucleus space of these HPLF samples. A diffuse distribution of clustered rod-like mitochondria was also detectable (Fig. 2A,B).

HPLFs in contact for 24h with 0.4 mm-thick bovine pericardium membranes (T2) displayed a large nucleus and a prominent nucleolus (Fig. 3A,B). There was also a peripheral localization of HE, while EU filled most of

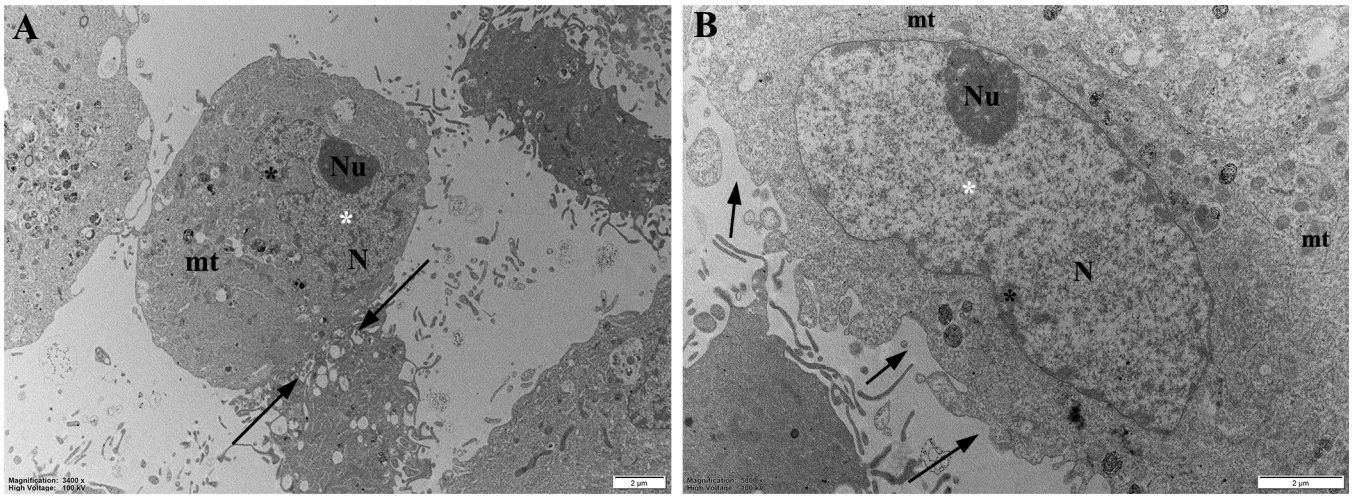

Fig. 1. Representative micrograph of hPLFs not exposed to bovine pericardium membranes (Ultrathin section: 80 m). **A.** hPLFs not exposed to bovine pericardium membranes showed a large nucleus (N), with a prominent nucleolus (Nu), and clustered mitochondria (mt). Heterochromatin (black asterix) and euchromatin (white asterix) are within the nucleus. Cytoplasmatic projections were also detectable (arrows). **B.** The ultrastructure of hPLFs not exposed to bovine pericardium membranes is characterized by a large nucleus (N), a prominent nucleolus (Nu), clustered mitochondria (m), and cytoplasmatic projections (arrows). Heterochromatin (black asterix) and euchromatin (white asterix) were visible in the nucleus. Scale Bars: 2 μm.

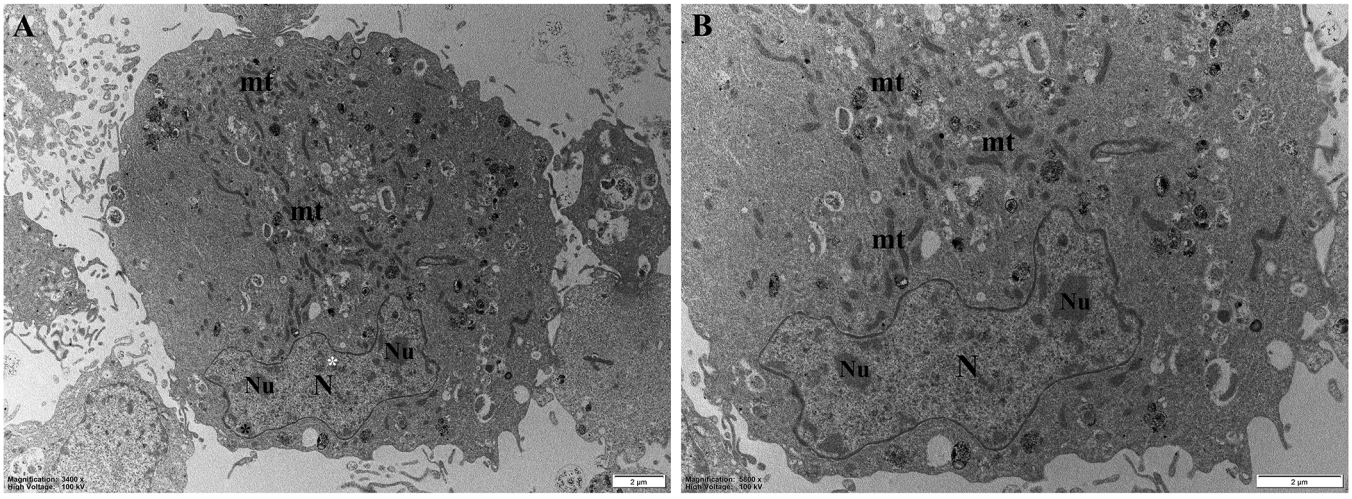

Fig. 2. Representative micrograph of hPLFs in contact for 24h with bovine pericardium membranes (thickness: 0.2 mm) (Ultrathin section: 80 nm): **A.** hPLFs exposed to bovine pericardium membranes showed a large nucleus (N), two prominent nucleolus (Nu), and a diffuse distribution of clustered rod-like shaped mitochondria (m). Heterochromatin (black asterix) and euchromatin (white asterix) were within the nucleus. **B.** The ultrastructure of hPLFs exposed to bovine pericardium membranes was characterized by a large nucleus (N), and prominent nuelolus (Nu). Mitochondria, which displayed a rod-like shape, showed a diffuse localization. Scale Bars: 2 μm.

the nucleus space (Fig. 3A,B). Clustered rod-like mitochondria were also visible in HPLFs exposed to bovine pericardium membranes (T2). Furthermore, richly developed ER and Golgi apparatus (Fig. 3A,B) were also detected in HPLFs exposed to T2 bovine pericardium membranes. Finally, the development of extensive tapering cytoplasmic projections (Fig. 3A,B) was also reported using TEM in HPLF samples exposed to T2 bovine pericardium membranes.

Morphometric and statistical analyses: Significant mitochondrial number increases with both membranes

Morphometric and statistical evaluations on semithin and ultrathin sections revealed that the number of mitochondria increased in HPLFs exposed for 24 hours to bovine pericardium membranes with different thicknesses (T1 and T2). The morphometric analysis revealed an upward trend in the number of mitochondria from the control group to HPLFs exposed to different bovine pericardium membranes, as resumed in Table 1. As shown in Figure 4, a significant increase was evidenced between controls and T1 (89.23±7.44 vs. 66.90±9.58, respectively; $p<0.01$) (Table 2) and T2 (T2: 84.05±14.01 vs. 66.90±9.58, respectively; $p<0.05$) (Table 2). No difference was found between T1 and T2.

Discussion

The scaffold triggered ultrastructural changes in HPLFs

TEM observations revealed ultrastructural changes in HPLFs when exposed for 24 hours to bovine pericardium membranes, for both thicknesses. Previous investigations using LM (Ivanovski et al., 2001; Marchetti et al., 2020; Bianchi et al., 2021) and scanning electron microscopy (SEM) detected the well-defined fusiform morphology and small dimensions of HPLFs after 24-hour contact with bovine pericardium membranes (thickness: 0.2 and 0.4 mm), with a flattened and elongated shape (Thomas and Gupta, 2017); however, there is a lack of scientific evidence of the ultrastructural changes that characterized HPLFs,

Table 1. Morphometric evaluation of the number of mitochondria in HPLFs not exposed for 24 hours to bovine pericardium membranes (control group), HPLFs exposed for 24 hours to bovine pericardium membranes (T1 - thickness: 0.2 mm) and HPLFs in contact for 24 hours with bovine pericardium membranes (T2 - thickness: 0.4 mm). Values are expressed as mean ± SD.

	Control group	T1	T2
N° of mitochondria/100 μm^2	66.90±9.58	89.23±7.44	84.05±14.01

Table 2. Summary of the one-way ANOVA with Tukey's honest significant difference (HSD) test considering the exposure to the different materials.

	Turkey's Multiple Comparisons Test		
	Mean Diff.	95.00% CI of diff.	*p* value
Control group vs T1	-22.33	-38.38 to -6.29	0.006
Control group vs T2	-17.16	-33.21 to -1.11	0.03
T1 vs T2	5.18	-10.87 to 21.22	ns

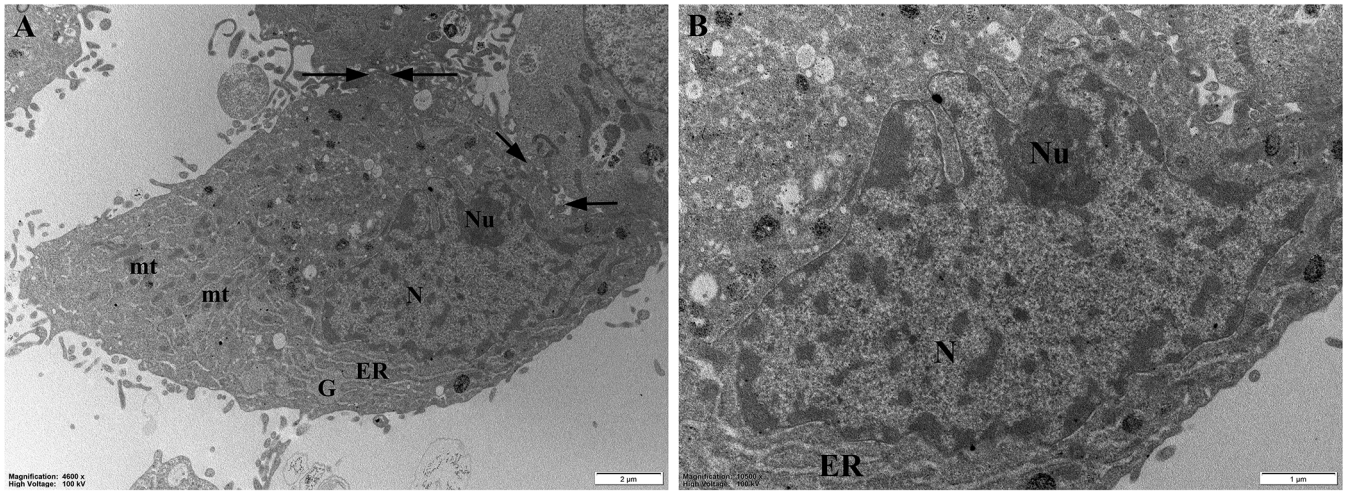

Fig. 3. Representative micrograph of hPLFs in contact for 24h with bovine pericardium membranes (thickness: 0.4 mm (Ultrathin section: 80 nm): **A.** hPLFs exposed to bovine pericardium membranes showed a big heterochromatic nucleus (N), with a prominent nucleolus (Nu). Clustered and rod-like shaped mitochondria (mt), endoplasmic reticulum (ER) and Golgi apparatus (G) were also detectable. The ultrastructure of hPLFs is also chracterized by cytoplasmatic projections (arrow). **B.** hPLFs in contact with bovine pericardium membranes display a big eterochromatic nucleus (N), with a prominent nucleolus (Nu), and visible endoplasmic reticulum (ER). Scale Bars: A, 2 μm; B, 1 μm.

specifically when exposed to regenerative biomaterials. In this study, the use of TEM allowed us to explore the ultrastructure (Sakaew et al., 2023) of this cell population by defining the distribution and quality of specific parameters: nucleus, nucleolus, mitochondria, ER, and Golgi apparatus. In our TEM observations, the presence of multiple prominent nucleoli was particularly noteworthy, probably associated with an intense synthesis of ribosomal RNA (rRNA) and suggestive of cellular protein synthesis activity (Repiská et al., 2010). The nucleolus is the site of ribosome biogenesis (Correll et al., 2019), as within this compartment, rRNAs are synthesized, processed, and assembled with ribosomal proteins (Patrasso et al., 2023). Recent studies reported the upregulation of RNA levels of osteogenic genes (*RUNX2*, *BMP2*) in human periodontal ligament stem cells (hPDLSCs) in culture with bovine pericardium collagen membranes (Pizzicanella et al., 2019). Bovine pericardial membranes express different functional and structural proteins, with a significant implication for osteogenesis and collagen fibrillogenesis, impacting their frequent use as regenerative biomaterials (Hirata et al., 2015). As also shown by earlier studies (Hynes, 2002; Masci et al., 2016; Li et al., 2021), when fibroblasts are co-cultured with collagen scaffold, the collagen fibers mimic the extracellular matrix (ECM). The contact of the scaffolds with the cellular surface activates integrin proteins, stimulating the metabolic pathway of fibroblasts, including degradation and new collagen synthesis (Hynes, 2002).

The active synthetic state of HPLFs is confirmed by the presence of a prominent contrasted structure of the cell nucleus and by the distribution of EU, which filled most of the nucleus space, suggestive of a transcriptionally active stage of the selected cell population (Repiská et al., 2010). Furthermore, our observations also reported the presence of abundant and richly developed ER in HPLFs exposed to bovine pericardium membranes (T2), suggestive of the active state (Repiská et al., 2010) and mature stage of development of fibroblasts (Dard et al., 1989). Interestingly, a highly developed Golgi apparatus was found in cultures exposed to 0.4 mm-thick membranes for 24 hours. This cytoplasmic organelle is responsible for the glycosylation of proteins and the synthesis of molecular components of the ground interfibrillar substance of the ECM (Zerbinati et al., 2017). For these reasons, the intense development of these specific ultrastructural features (ER and Golgi apparatus) is suggestive of triggering and activation of the selected cell population in the renewal/remodeling processes of connective tissue by promoting the synthesis of new molecular components of the ECM (Zerbinati et al., 2017). Furthermore, the exposure of HPLFs to bovine pericardium membranes determined the development of clustered rod-like mitochondria, suggestive of a functional state, as expected in live cells (Van Der Merwe et al., 2014, Hirashima et al., 2020). Moreover, morphometric and statistical analyses reported an upward trend in the number of mitochondria from the control group to HPLFs exposed to different bovine pericardium membranes (Tables 1, 2, Fig. 4).

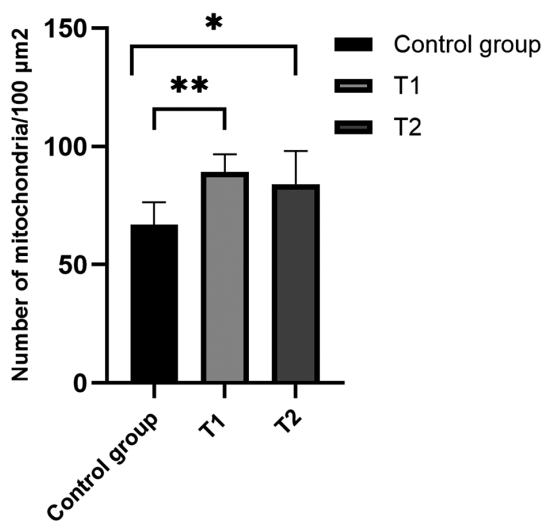

Fig. 4. Quantitative analysis of mitochondria number in HPLFs. Control group: HPLFs cultured for 24 hour and not exposed to bovine pericardium membranes. T1: HPLFs exposed for 24 hours to bovine pericardium membranes, characterized by a thickness of 0.2 mm. T2: HPLFs in contact for 24 hours with bovine pericardium membranes, with a thickness of 0.4 mm. All data were presented as mean ‡ SD, *p<0.05; **p<0.01.

The lack of scientific evidence regarding the numerical density of these cellular organelles in HPLFs, precisely when in contact with regenerative biomaterials, defines our preliminary results. This highlighted the need to extend the window of time (e.g., 72 hours and 7 days) to perform morphometric and statistical analyses at different follow-up times. However, despite the preliminary nature of the data, the ultrastructural evidence indicated that the exposure of HPLFs to bovine pericardium membranes of varying thicknesses may stimulate fibroblast activity, supporting their essential and dynamic role in regenerative processes.

Implications of ultrastructural observations in the use of bovine pericardium membrane

In our earlier study, we examined the external morphology and proliferation of HPLFs in contact with bovine pericardium membranes with different thicknesses (0.2 and 0.4 mm) and at three different follow-ups (24 hours, 72 hours, and 7 days) (Bianchi et al., 2022b). The results showed how the studied membranes increase cellular proliferation and stimulate cellular reactions with the development of cytoplasmic projections (Mehta et al., 2018), which agrees with the evidence in the literature. Indeed, in 2016, Masci et al. found that fibroblasts co-cultured with collagen I fibers develop intracellular vacuoles and filipodia to embed the fibers and shed microvesicles to degrade the collagen

scaffold (Masci et al., 2016), fundamental stages for any regenerative process including the periodontal one. Regarding the exposure to regenerative biomaterials, in their *in vitro* study, Nguyen et al. showed that 24 hours of exposure to bovine pericardium membranes (thickness range: 0.2–0.5 mm) induced attachment, migration, and proliferation in human GFs (Nguyen and Tran, 2018). These features associated with proliferative and migration patterns are also confirmed in HPLFs, whose ultrastructure displayed extensive cytoplasmic projections after 24 hours of exposure to bovine pericardium membranes of 0.4 thickness (Fig. 3).

The thickness of the membrane has been shown to play a crucial role in *in vivo* studies using animal models (Bubalo et al., 2012; Lee et al., 2017). In particular, Bubalo et al. (2012) found that thicker membranes were less performative than those of less thickness. Those results were attributed to the diminished capacity of ion channel passage due to the higher thickness (Lee et al., 2017). According to recent scientific evidence, the collagen-rich ECM, a natural and hospitable micro-environment that characterizes bovine pericardium membranes, mainly contributes to the onset and progression of cellular migration, proliferation, and regeneration (Mehta et al., 2018).

Atar et al. (2014) assessed the morphology of HPLFs cultured on bovine pericardium membranes using SEM analysis. The cells exhibited a flattened appearance as cellular processes developed.

The bovine pericardium has historically been used for regenerative and prosthetic purposes (Mehta et al., 2018). Due to the presence of a collagen-rich ECM, which determines the material's flexibility, bovine pericardium membranes are fundamental to creating the best environmental conditions for regenerative surgery (Mehta et al., 2018). Moreover, different histological studies on bovine pericardium membranes demonstrated that pericardial tissue has the best mechanical or physical properties in different medical contexts (Choe et al., 2018). Several recent studies (Repiská et al., 2010; Mehta et al., 2018; Shi et al., 2023; Huang et al., 2023) suggested that bovine pericardium membranes are highly biocompatible with human fibroblasts and HPLFs (Setyawati et al., 2020), by providing the necessary scaffold for periodontal ligament fibroblast attachment (Chang et al, 2023), collagen synthesis, migration, and proliferation (Hirata et al., 2015), and are therefore, successfully applied for periodontal regeneration (Shin and Sohn, 2005; Chang et al., 2023). Although there is a lack of functional and ultrastructural data regarding the synthesis of collagen and proteins involved in regeneration, this TEM evidence sheds light on the active synthetic state of HPLFs after 24 hours of exposure to bovine pericardium membranes of different thicknesses. Specifically, the ultrastructural changes described in this study suggested an active synthetic state of HPLFs, which probably prepares this cell population for future collagen synthesis associated with tissue regeneration. Nonetheless, further molecular and ultrastructural investigations are needed to fully understand the mechanisms behind this interaction. Furthermore, the ultrastructural data from our TEM study confirm how the interaction between bovine pericardium membranes and HPLFs stimulates cytoskeletal changes, cell proliferation, and enhanced metabolic activity.

These results indicate the use of bovine pericardium as an appropriate material, which stimulates not only the adhesion, migration, and proliferation but also the metabolic activity of fibroblasts in periodontal regenerative procedures.

Strengths and limitations

The primary strength of this study lies in the use of TEM to describe the impact of bovine pericardium membranes on the ultrastructure of HPLFs. While previous research focused on the effects of these regenerative biomaterials on the viability and proliferation of HPLFs (Bianchi et al., 2022a,b), this study uniquely provides an ultrastructural view of the interaction between HPLFs and these membranes.

However, several limitations characterized this study, including the applied protocol, sample size, follow-up period, and the absence of a morpho-functional investigation. The applied protocol probably impacted the results presented, using established but not advanced technique protocols such as Automated Live Cell Analysis, Scanning-Transmission Electron Microscopy, and Correlative Microscopy. This limitation, however, suggests the future use of more advanced and complementary microscopy techniques, strengthening the data presented.

At the same time, the sample size might have constrained the significance of observed differences, despite the results of the quantitative analysis of mitochondrial organelles in TEM images. Additionally, the short follow-up period was a further limitation, suggesting that extending exposure times (e.g., 72 hours and 7 days) would benefit the future of this research. Regarding molecular investigations, a future interesting perspective of this study might be the association of changes in cellular content (ultrastructural morphology) with molecular analysis of human GF or HPLF cell adhesion to the membrane. Finally, the study reported an active synthetic state of HPLFs exposed to bovine pericardium membranes, presumably predisposing this cell population to the future synthesis of proteins associated with tissue regeneration. Considering this hypothesis, a further area for exploration would be to expand the morpho-functional investigation by correlating the ultrastructural findings with the expression of protein synthesis markers involved in the regenerative process.

Conclusion

HPLFs exposed to bovine pericardium membranes

of varying thicknesses exhibited distinct ultrastructural changes in specific organelles. Specifically, the presence of a large nucleus with different prominent nucleoli suggests intense protein synthesis in HPLFs exposed to the tested materials. At the same time, the presence of clusters of mitochondria and richly developed ER confirmed the active functional and mature stage of this cell population when exposed to bovine pericardium membranes of varying thicknesses. The active synthetic state of HPLFs revealed in this study probably favors this cell population to synthesize proteins related to tissue regeneration. Finally, these ultrastructural details offer valuable insights into the cellular architecture of HPLFs, which may help clarify microenvironmental changes during the regeneration process.

Author Contributions. Conceptualization, Sara Bernardi and Enrico Marchetti; methodology, Davide Simeone and Diana Torge; validation, Sara Bernardi and Serena Bianchi; formal analysis, Diana Torge; investigation, Davide Simeone and Diana Torge; resources, Enrico Marchetti and Guido Macchiarelli; writing, original draft preparation, Diana Torge and Davide Simeone; writing, review and editing, Serena Bianchi, Guido Macchiarelli, and Enrico Marchetti; supervision, Serena Bianchi, Guido Macchiarelli, and Enrico Marchetti; project administration, Sara Bernardi; funding acquisition, Serena Bianchi, Guido Macchiarelli, and Enrico Marchetti. All authors have read and agreed to the published version of the manuscript.

Funding. This research received no external funding.

Conflicts of Interest. The authors declare no conflict of interest.

References

Arjunan A., Baroutaji A., Robinson J., Praveen A.S., Pollard A. and Wang C. (2021). Future directions and requirements for tissue engineering biomaterials. In: Encyclopedia of smart materials. Olab A.-G. (ed). pp 195-218.

Athar Y., Zainuddin S.L.A., Berahim Z., Hassan A., Sagheer A. and Alam M.K. (2014). Bovine pericardium membrane and periodontal guided tissue regeneration: A SEM study. Int. Med. J. 21, 325-327.

Bai M., Zhang T., Ling T., Zhou Z., Xie H., Zhang W., Hu G., Jiang C., Li M., Feng B. and Wu H. (2014). Guided bone regeneration using acellular bovine pericardium in a rabbit mandibular model: in-vitro and in-vivo studies. J. Periodontal Res. 49, 499-507.

Bianchi S., Mancini L., Torge D., Cristiano L., Mattei A., Varvara G., Macchiarelli G., Marchetti E. and Bernardi S. (2021). Bio-Morphological reaction of human periodontal ligament fibroblasts to different types of dentinal derivates: *In vitro* study. Int. J. Mol. Sci. 22, 8681.

Bianchi S., Bernardi S., Mattei A., Cristiano L., Mancini L., Torge D., Varvara G., Macchiarelli G. and Marchetti E. (2022a). Morphological and biological evaluations of human periodontal ligament fibroblasts in contact with different bovine bone grafts treated with low-temperature deproteinisation protocol. Int. J. Mol. Sci. 23, 5273.

Bianchi S., Bernardi S., Simeone D., Torge D., Macchiarelli G. and Marchetti E. (2022b). Proliferation and morphological assessment of human periodontal ligament fibroblast towards bovine pericardium membranes: An *in vitro* study. Materials 15, 8284.

Bubalo M., Lazić Z., Matić S., Tatić Z., Milović R., Curcin A.P., Djurdjević D. and Loncarević S. (2012). The impact of thickness of resorbable membrane of human origin on the ossification of bone defects: a pathohistologic study. Vojnosanit. Pregl. 69, 1076-1083.

Burattini S. and Falcieri E. (2013). Analysis of cell death by electron microscopy. Methods Mol. Biol. 1004, 77-89.

Chang Y.T., Lai C.C. and Lin D.J. (2023). Collagen scaffolds laden with human periodontal ligament fibroblasts promote periodontal regeneration in SD rat model. Polymers 15, 2649.

Choe J.A., Jana S., Tefft B.J., Hennessy R.S., Go J., Morse D., Lerman A. and Young M.D. (2018). Biomaterial characterization of off-the-shelf decellularized porcine pericardial tissue for use in prosthetic valvular applications. J. Tissue. Eng. Regen. Med.12, 1608-1620.

Coaguila-Llerena H., Ochoa-Rodríguez V.M., Passos Barbieri I., Ramos S.G. and Faria G. (2024). Calcium hypochlorite cytotoxicity mechanism in fibroblasts and effect on osteoblast mineralization. Int. Endod. J. 57, 64-77.

Correll C.C., Bartek J. and Dundr M. (2019). The nucleolus: A multiphase condensate balancing ribosome synthesis and translational capacity in health, aging and ribosomopathies. Cells 8, 869.

Dard M., Kerebel L.M. and Kerebel B. A. (1989). Transmission electron microscope study of fibroblast changes in human deciduous tooth pulp. Arch. Oral. Biol. 34, 223-228.

Elboraey M.O. and Mously E.A. (2023). Clinical and radiographic evaluation of third-generation pericardium membrane for the treatment of grade II furcation defect in stage III periodontitis patients. Medicina 59, 572.

Gates K.V., Dalgliesh A.J. and Griffiths L.G. (2017). Antigenicity of bovine pericardium determined by a novel immunoproteomic approach. Sci. Rep. 7, 2446.

Griesemer A., Yamada K. and Sykes M. (2014). Xenotransplantation: immunological hurdles and progress toward tolerance. Immunol. Rev. 258, 241-258.

Hirashima S., Kanazawa T., Ohta K. and Nakamura K. (2020). Three-dimensional ultrastructural imaging and quantitative analysis of the periodontal ligament. Anat. Sci. Int. 95, 1-11.

Hirata H.H., Munhoz M.A.S., Plepis A.M.G., Martins V.C.A., Santos G.R., Galdeano E.A. and Cunha M.R. (2015). Feasibility study of collagen membranes derived from bovine pericardium and intestinal serosa for the repair of cranial defects in ovariectomised Rats. Injury 46, 1215-1222.

Huang L., Chen L., Chen H., Wang M., Jin L., Zhou S., Gao L., Li R., Li Q., Wang H., Zhang C. and Wang J. (2023). Biomimetic scaffolds for tendon tissue regeneration. Biomimetics 8, 246.

Hynes R.O. (2002). Integrins: Bidirectional, allosteric signaling machines. Cell 110, 673-687.

Ivanovski S., Li H., Haase H.R. and Bartold P.M. (2001). Expression of bone associated macromolecules by gingival and periodontal ligament fibroblasts. J. Periodontal. Res. 36, 131-141.

Lee Y.J., An S.J., Bae E.B., Gwon H.J., Park J.S., Jeong S.I., Jeon Y.C., Lee S.H., Lim Y.M. and Huh J.B. (2017). The effect of thickness of resorbable bacterial cellulose membrane on guided bone regeneration. Materials 10, 320.

Leoni G.G., Palmerini M.G., Satta V., Succu S., Pasciu V., Zinellu A., Carru C., Macchiarelli G., Nottola S.A., Naitana S. and Berlinguer F. (2015). Differences in the kinetic of the first meiotic division and in active mitochondrial distribution between prepubertal and adult oocytes mirror differences in their developmental competence in a sheep model. PLoS One 10, e0124911.

Li W., Chi N., Rathnayake R.A.C. and Wang R. (2021). Distinctive roles

of fibrillar collagen I and collagen III in mediating fibroblast-matrix interaction: A nanoscopic study. Biochem. Biophys. Res. Commun. 560, 66-71.

Liu Z.Z., Wong M.L. and Griffiths L.G. (2016). Effect of bovine pericardial extracellular matrix scaffold niche on seeded human mesenchymal stem cell function. Sci. Rep. 6, 37089.

Manji R.A., Zhu L.F., Nijjar N.K., Rayner D.C., Korbutt G.S., Churchill T.A., Rajotte R.V., Koshal A. and Ross D.B. (2006). Glutaraldehyde-fixed bioprosthetic heart valve conduits calcify and fail from xenograft rejection. Circulation 114, 318-327.

Manji R.A., Lee W. and Cooper D.K.C. (2015). Xenograft bioprosthetic heart valves: Past, present and future. Int. J. Surg. 23 (Pt B), 280-284.

Masci V.L., Taddei A.R., Gambellini G., Giorgi F. and Fausto A.M. (2016). Ultrastructural investigation on fibroblast interaction with collagen scaffold. J. Biomed. Mater. Res. A 104, 272-282.

Marchetti E., Mancini L., Bernardi S., Bianchi S., Cristiano L., Torge D., Marzo G. and Macchiarelli G. (2020). Evaluation of different autologous platelet concentrate biomaterials: morphological and biological comparisons and considerations. Materials 13, 2282.

Mas-Moruno C., Su B. and Dalby M.J. (2019). Multifunctional coatings and nanotopographies: Toward cell instructive and antibacterial implants. Adv. Healthc. Mater. 8, e1801103.

Mehta D.B., Deshpande N.C. and Dandekar S.A. (2018). Comparative evaluation of platelet-rich fibrin membrane and collagen membrane along with demineralized freeze-dried bone allograft in Grade II furcation defects: A randomized controlled study. J. Indian Soc. Periodontol. 22, 322-327.

Mendoza-Novelo B., Avila E.E., Cauich-Rodríguez J.V., Jorge-Herrero E., Rojo F.J., Guinea G.V. and Mata-Mata J.L. (2011). Decellularization of pericardial tissue and its impact on tensile viscoelasticity and glycosaminoglycan content. Acta Biomater. 7, 1241-1248.

Murray G.F., Turner T.H., Leslie K.A., Alzubi M.A., Guest D., Sohal S.S., Teitell M.A., Harrell J.C. and Reed J. (2018). Live cell mass accumulation measurement non-invasively predicts carboplatin sensitivity in triple-negative breast cancer patient-derived xenografts. ACS Omega 3, 17687-17692.

Nguyen M.T.N. and Tran H.L.B. (2018). Effect of modified bovine pericardium on human gingival fibroblasts *in vitro*. Cells Tissues Organs. 206, 296-307.

Orioles M., Galeotti M., Saccà E., Bulfoni M., Corazzin M., Bianchi S., Torge D., Macchiarelli G., Magi G.E. and Schmidt J.G. (2022). Effect of temperature on transfer of midichloria-like organism and development of red mark syndrome in rainbow trout (Oncorhynchus Mykiss). Aquaculture 560, 738577.

Patrasso E.A., Raikundalia S. and Arango D. (2023). Regulation of the epigenome through RNA modifications. Chromosoma 132, 231-246.

Pizzicannella J., Marconi G.D., Pierdomenico S.D., Cavalcanti M.F.X.B., Diomede F. and Trubiani O. (2019). Bovine pericardium membrane, gingival stem cells, and ascorbic acid: a novel team in regenerative medicine. Eur. J. Histochem. 63, 3064.

Repiská V., Varga I., Lehocký I., Böhmer D., Blaško M., Polák Š., Adamkov M. and Danišovič Ľ. (2010). Biological and morphological characterization of human neonatal fibroblast cell culture B-HNF-1. Biologia 65, 919-24.

Sakaew W., Somintara S., Jongsomchai K., El-Abid J., Wongprasert K., Kovensky J. and Rudtanatip T. (2023). Octanoyl esterification of low molecular weight sulfated galactan enhances the cellular uptake and collagen expression in fibroblast cells. Biomed. Rep. 19, 99.

Setyawati E.M. and Klana N.A.P. (2020). Concise review: Periodontal tissue regeneration using pericardium membrane as guided bone regeneration. AIP Conf. Proc. 2314, 050015.

Shi X., Li X., Tian Y., Qu X., Zhai S., Liu Y., Jia W., Cui Y. and Chu S. (2023). Physical, mechanical, and biological properties of collagen membranes for guided bone regeneration: A comparative *in vitro* study. BMC Oral Health 23, 510.

Shin H.I. and Sohn D.S. (2005). A method of sealing perforated sinus membrane and histologic finding of bone substitutes: A case report. Implant. Dent. 14, 328-333.

Simon P., Kasimir M.T., Seebacher G., Weigel G., Ullrich R., Salzer-Muhar U., Rieder E. and Wolner E. (2003). Early failure of the tissue engineered porcine heart valve SYNERGRAFT in pediatric patients. Eur. J. Cardiothorac. Surg. 23, 1002-106.

Soldatos N.K., Stylianou, P., Koidou, P., Angelov, N., Yukna, R. and Romanos, G.E. (2017). Limitations and options using resorbable *versus* nonresorbable membranes for successful guided bone regeneration. Quintessence Int. 48, 131-147.

Thomas B. and Gupta K. (2017). *In vitro* biocompatibility of hydroxyapatite-added GIC: An SEM study using human periodontal ligament fibroblasts. J. Esthet. Restor. Dent. 29, 435-441.

Torge D., Bernardi S., Ciciarelli G., Macchiarelli G. and Bianchi S. (2024). Dedicated protocol for ultrastructural analysis of farmed rainbow trout (*Oncorhynchus mykiss*) tissues with red mark syndrome: The skin-part one. Methods Protoc. 7, 37.

Vallecillo-Rivas M., Toledano-Osorio M., Vallecillo C., Osorio R. and Toledano M. (2021). The collagen origin influences the degradation kinetics of guided bone regeneration membranes. Polymers 13, 3007.

van der Merwe C., Loos B., Swart C., Kinnear C., Henning F., van der Merwe L., Pillay K., Muller N., Zaharie D., Engelbrecht L., Carr J. and Bardien S. (2014). Mitochondrial impairment observed in fibroblasts from South African Parkinson's disease patients with parkin mutations. Biochem. Biophys. Res. Commun. 447, 334-340.

Wang R., Bao B., Bao C., Wang S., Ur Rahman S., Hou C., Elango J. and Wu W. (2020). Resveratrol and celastrol loaded collagen dental implants regulate periodontal ligament fibroblast growth and osteoclastogenesis of bone marrow macrophages. Chem. Biodivers. 17, e2000295.

Zerbinati N., D'Este E., Parodi P.C. and Calligaro A. (2017). Microscopic and ultrastructural evidences in human skin following calcium hydroxylapatite filler treatment. Arch. Dermatol. Res. 309, 389-396.

Zioupos P. and Barbenel J.C. (1994). Mechanics of native bovine pericardium. I. The multiangular behaviour of strength and stiffness of the tissue. Biomaterials 15, 366-373.

Accepted December 12, 2024